AGU PUBLICATIONS

Geophysical Research Letters

RESEARCH LETTER
10.1002/2017GL074831

Key Points:
- Summer temperatures in the central U.S. are influenced by circulation and land surface conditions
- Circulation effects on summer temperatures can be removed with dynamical adjustment
- Residual temperature variability in the central U.S. reflects the land surface feedback

Supporting Information:
- Supporting Information S1

Correspondence to:
A. Merrifield,
almerrif@ucsd.edu

Citation:
Merrifield, A., Lehner, F., Xie, S.-P., & Deser, C. (2017), Removing circulation effects to assess central U.S. land-atmosphere interactions in the CESM Large Ensemble, *Geophysical Research Letters*, *44*. https://doi.org/10.1002/2017GL074831

Received 12 JUL 2017
Accepted 17 SEP 2017
Accepted article online 22 SEP 2017

Removing Circulation Effects to Assess Central U.S. Land-Atmosphere Interactions in the CESM Large Ensemble

Anna Merrifield[1], Flavio Lehner[2], Shang-Ping Xie[1], and Clara Deser[2]

[1]Scripps Institution of Oceanography, University of California, San Diego, CA, USA, [2]Climate and Global Dynamics Division, National Center for Atmospheric Research, Boulder, CO, USA

Abstract Interannual variability of summer surface air temperature (SAT) in the central United States (U.S.) is influenced by atmospheric circulation and land surface feedbacks. Here a method of dynamical adjustment is used to remove the effects of circulation on summer SAT variability over North America in the Community Earth System Model Large Ensemble. The residual SAT variability is shown to reflect thermodynamic feedbacks associated with land surface conditions. In particular, the central U.S. is a "hot spot" of land-atmosphere interaction, with residual SAT accounting for more than half of the total SAT variability. Within the "hot spot," residual SAT anomalies show higher month-to-month persistence through the warm season and a redder spectrum than dynamically induced SAT anomalies. Residual SAT variability in this region is also shown to be related to preseason soil moisture conditions, surface flux variability, and local atmospheric pressure anomalies.

1. Introduction

Adverse impacts from anthropogenic climate change are likely to be exacerbated in summer when temperatures are already at their seasonal maximum. Indeed, exceptionally warm summers projected by climate models will jeopardize crops, strain water resources, and tax human health (Romero-Lankao et al., 2014; Lehner, Wahl, et al., 2017). With a surfeit of solar radiation present, summer SAT over land is set by large-scale atmospheric circulation patterns, topography, and cloud cover and modified regionally by land surface conditions.

The land surface influences the atmosphere through a series of nonlinear processes, linking soil moisture with evapotranspiration, cloud formation and precipitation (e.g., Findell & Eltahir, 2003; Tawfik et al., 2015a, 2015b). Modeling studies identify a "hot spot" of land-atmosphere interaction in the central U.S. (e.g., Koster et al., 2006; Lorenz et al., 2015; Zhang et al., 2008). There are indications, however, that the land-atmosphere coupling in such hot spot regions might be overestimated in climate models (Fischer et al., 2012; Sippel et al., 2017; Stegehuis et al., 2013). In the central U.S., for example, models tend to feature warmer mean SAT (Mueller & Seneviratne, 2014) and more interannual SAT variability (Berg et al., 2014; Merrifield & Xie, 2016) than observed. The land surface influence on SAT is challenging to quantify (Yang et al., 2004) due to the confounding influence of internal atmospheric variability (Deser et al., 2012; Wallace et al., 1995, 2015). For example, hot extremes brought about by persistent anticyclonic conditions in the atmosphere are often intensified by dry soils (Durre et al., 2000; Miralles et al., 2014; Vogel et al., 2017).

This study uses the empirical method of "dynamical adjustment" (Deser et al., 2016; Lehner, Deser, et al., 2017) to remove the circulation-induced component of SAT variability in the Community Earth System Large Ensemble. We examine the relative magnitude, spatial pattern, and temporal persistence of circulation versus thermodynamic drivers of summer SAT variability over the U.S., with particular attention on the central U.S. hot spot region identified in previous studies. Specifically, we evaluate whether the thermodynamic component of SAT variability helps isolate influences of anomalous land surface conditions. The remainder of the paper is structured as follows. Section 2 introduces the model simulations and dynamical adjustment methodology. Results are presented in Section 3, beginning with two case studies and then generalizing to characterize the dynamic and thermodynamic contributions to SAT variability in the Community Earth System Model Large Ensemble. Sections 4 and 5 provide a summary and discussion, respectively.

2. Climate Model Simulations and Dynamical Adjustment Methodology

We analyze the role of the atmospheric circulation and land surface condition on summer SAT variability over the historical period (1920–2005) in the 30 member ensemble of simulations conducted with the National Center of Atmospheric Research (NCAR) Community Earth System Model version 1 (CESM1), hereafter referred to as the CESM Large Ensemble (CESM-LE) (Kay et al., 2015). The CESM-LE is a fully coupled, 1° horizontal resolution initial condition ensemble; each ensemble member is subjected to identical CMIP5-based external forcing scenarios. The members differ slightly from one another in their initial atmospheric state. Large ensembles allow us to sample internal variability in the presence of forced climate changes, thereby providing a range of possible climate trajectories to analyze (Deser et al., 2012; Lehner et al., 2016).

We employ constructed circulation analogues to dynamically adjust monthly mean SAT fields in the CESM-LE. The method is summarized briefly here and in more detail in the supporting information; the reader is referred to Deser et al. (2016) for a full description.The method relies on the ability to reconstruct a given monthly mean circulation field ("target month"), represented here by monthly mean 500 mb geopotential height (Z500) as opposed to SLP as in Deser et al. (2016), from a large set of imperfect analogues obtained from the CESM1 preindustrial control simulation (Kay et al., 2015) with the same model setup. The closest analogues (in terms of Euclidean distance from the target month over the domain 20–90°N, 180–10°W) are linearly combined with an optimal set of weights, to reconstruct the target Z500 field in the CESM-LE. The same optimal linear combination is then applied to the accompanying SAT fields in the control simulation to construct the dynamically induced component of SAT. This dynamical component is then subtracted from the original SAT field of the target month to obtain the residual SAT component, which we interpret as being primarily thermodynamically induced and potentially land surface driven.

3. Results

3.1. Two Julys With Similar Circulation but Different SAT

In the central U.S., different SAT anomalies can exist under similar atmospheric circulation conditions (Figure 1). To illustrate this, we select two Julys from the CESM-LE (July 1963 of member 15, and July 1925 of member 22) featuring similar midlatitude bands of high pressure at 500 hPa (Z500) with centers in the vicinity of the Aleutian islands and the west coast of the U.S. and a low-pressure center over western Canada, similar to the pattern described by McKinnon et al. (2016). SAT anomalies in the two cases differ most notably in the central U.S., while they are broadly similar elsewhere. The configuration of SAT anomalies associated with the Z500 pattern indicate that atmospheric circulation anomalies are largely responsible for the warm (cool) anomalies in the western U.S. (Canada) (Figures 1c and 1d). The local warm anomaly over the central U.S. in case 2 (Figure 1f), which exceeds average central U.S. SAT by more than 5°C, is not accounted for by dynamical adjustment and might hence be of thermodynamic origin. In contrast, there is no significant central U.S. SAT anomaly present in case 1 (Figure 1e). To investigate possible mechanisms explaining the differences in residual SAT anomaly over the central U.S., we compare area-averaged land surface parameters in the region shown in Figures 1e and 1f (32.5–41.9°N, 90–101.25°W). We consider soil moisture, sensible and latent heat fluxes, the shortwave cloud radiative effect, which is the difference between all-sky and clear-sky downward shortwave radiation at the surface (Cheruy et al., 2014), and the diurnal temperature range, which serves as proxy for local boundary layer moisture conditions (Dai et al., 1999; Lewis & Karoly, 2013). The land surface anomalies are presented in terms of percent difference from their long-term averages.

In case 1 (green bars in Figure 1g), soils are 4% wetter than average. The surface heat flux is partitioned in favor of latent (8%) over sensible (−14%) heating. Local atmospheric conditions were largely unremarkable, with modest reductions in cloud cover (−11%) and diurnal temperature range (−2%). In case 2 (blue bars in Figure 1g), soils are 11% drier than average. Anomalously dry soil conditions exist in the previous spring in case 2, from a −4% anomaly in April to a −10% anomaly in June (not shown). The sensible heat flux in the region is more than twice the long-term average (102%), in conjunction with a 25% reduction in the latent heat flux due to drier soils. Cloud cover is below average in case 2 (−30%), which suggests that the increase of incoming shortwave radiation that accompanies reductions in cloud cover contribute to the SAT anomaly in the region. The diurnal temperature range is 30% larger than average, which is consistent with drier boundary layer conditions that result in enhanced radiative warming during the day and cooling at night. The residual SAT anomaly in case 2 likely originated from heat flux partitioning by the land surface with reduced cloud cover playing a role, a narrative consistent with other case studies (e.g., Namias, 1982; Orth & Seneviratne, 2017; Perkins, 2015).

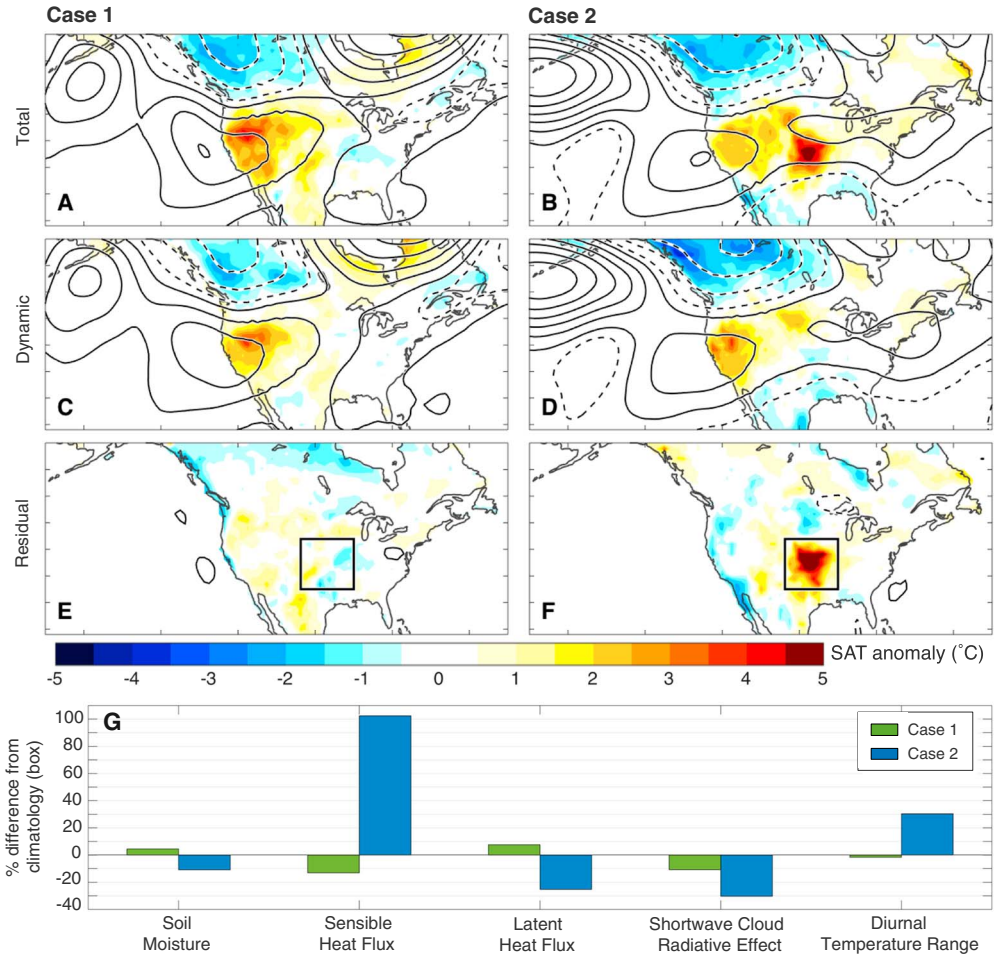

Figure 1. (a, b) Total, (c, d) dynamical, and (e,f) residual SAT anomalies (color) in two Julys with similar attendant circulation (Z500; contours) in the CESM-LE. Anomalies are calculated from the historical period mean (1920–2005). Z500 contours range from 5 to 95 m (solid) and −5 to −50 m (dashed) in 15 m intervals. (g) Area-averaged surface conditions for each July, expressed as percent difference from the historical period mean.

3.2. Defining the Hot Spot

The selected cases in Figure 1 demonstrate how residual SAT can help to identify the spatial extent and estimate the magnitude of the land surface's influence on summer SAT. To take a more general look at the SAT variability that might be driven by land surface conditions, we calculate the standard deviation (σ) of dynamic and residual SAT anomalies across all summers (June–August; JJA) of the historical portion of each member of the CESM-LE and then average the 30 σ values. Note that for each year and grid point, the ensemble-mean dynamic (residual) SAT has been subtracted from each ensemble member's dynamic (residual) SAT before computing σ, thereby isolating the contribution from internal variability. Interannual variability of dynamic JJA SAT in the CESM-LE is of comparable magnitude over the western and central U.S., though dynamics explain over three quarters of the total SAT σ in the former and less than half in the latter region (Figure 2a). Residual JJA SAT variability is highest along the arc of the Great Plains with almost no residual variability in the western U.S. (Figure 2b). The lack of residual σ west of the Rocky Mountains is consistent with the region being too dry overall for moisture variations to influence SAT (Kamae et al., 2016; Seneviratne et al., 2010). In the central U.S., the magnitude of residual variability suggests that the land surface feedbacks may be responsible for more than a quarter of total SAT σ. The southern central US (32.5–41.9°N, 90–98.75°W) stands out as a "hot spot," with more than half of the total SAT σ considered thermodynamic. Hereafter, SAT averaged over this region is defined as hot spot SAT.

The land surface's influence on SAT can also be inferred from temporal characteristics of dynamic and residual SAT within the hot spot region. Evidence of the land surface feedback can be seen on intraseasonal

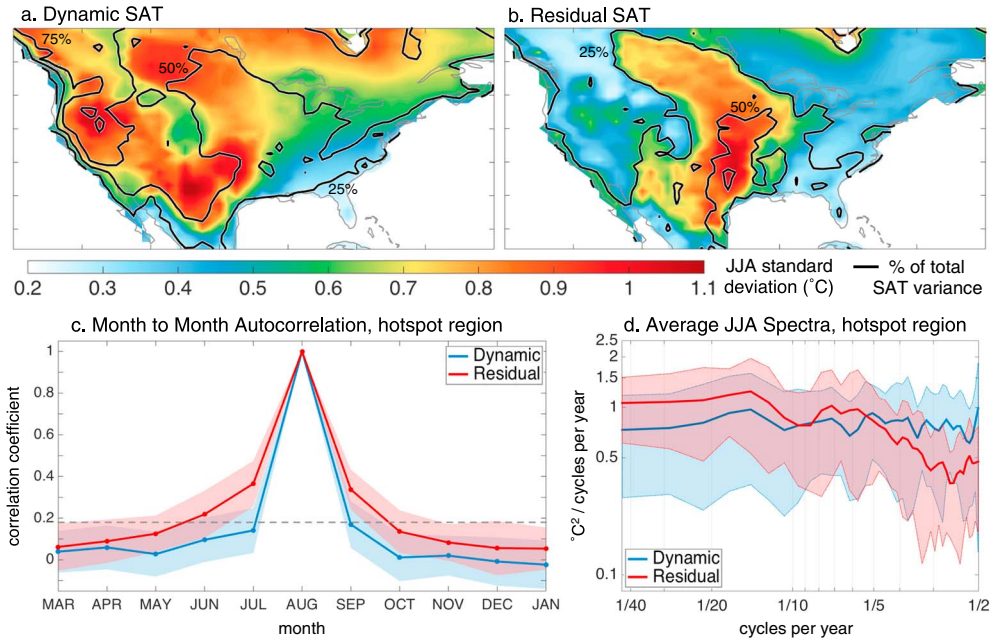

Figure 2. Standard deviation of (a) dynamic and (b) residual JJA SAT in color, overlaid with percent of total JJA SAT variance explained in black contours, averaged across 30 members of CESM-LE over the historical period. (bottom) Temporal features of hot spot region dynamic (blue) and residual (red) SAT. (c) August hot spot SAT autocorrelation and (d) spectra of JJA hot spot SAT, in terms of ensemble average (solid line) and 1σ ensemble spread (shading).

(Figure 2c) to multidecadal (Figure 2d) timescales. Autocorrelation of dynamic (blue) and residual (red) August SAT anomalies are shown in Figure 2c, where the solid curve shows the average and the shading shows the range across the 30 members of the CESM-LE. Although there is considerable spread in autocorrelations among the 30 model runs for both dynamic and residual SAT, on average, residual SAT has a longer decorrelation timescale than dynamic SAT. Residual autocorrelation significant at 95% (above gray dashed line in Figure 2c, see supporting information) arises in June and continues until September, which suggests that residual SAT originates from a persistent surface forcing which exerts influence throughout the warm season. Dynamic SAT reflects the shorter-lived influence of atmospheric circulation that is not significantly correlated from month to month. The spectra of dynamic (blue) and residual (red) JJA SAT anomalies over the 86 year historical period are shown in Figure 2d, where the solid curve shows the average and the shading shows the range across the ensemble. The spectrum of dynamic JJA SAT has approximately equal power at all frequencies, while the spectrum of residual JJA SAT has more energy at lower frequencies. The redder residual spectrum is consistent with the notion that residual SAT reflects the integration of stochastic atmospheric forcing by the land surface (Delworth & Manabe, 1993).

3.3. Developing a Thermodynamic Narrative

The above results suggest that residual SAT variability in the hot spot region might be land surface driven. Within the model, we can attempt to develop a thermodynamic narrative for this land surface influence. We explore several aspects of the land surface feedback in the JJA SAT hot spot region: the relationship between SAT and soil moisture (Figure 3) and between SAT and local SLP (Figure 4). We quantify the former by showing correlation maps of the components of JJA hot spot SAT and total soil moisture from the antecedent spring through the subsequent fall (Figure 3). Correlations (r) are computed from a concatenated record of 2,580 model years (30 simulations, 86 years each) and are determined to be significant at 95% if they exceed about 0.03 in absolute value (see supporting information). Total JJA hot spot SAT is negatively correlated with spring (March–May; MAM) soil moisture from the Gulf Coast through the central Great Plains (Figure 3i). The spatial structure of the correlation suggests that moist southerly flow from the Gulf provides the moisture necessary for the land surface to influence the atmosphere (Kushnir et al., 2010; Feng et al., 2011). The maximum of these lagged correlations ($r = -0.25$) occur in the southern portion of the hot spot. The average correlation of dynamic JJA hot spot SAT with MAM soil moisture in the hot spot is very low ($r = -0.05$; Figure 3ii), which suggests that the spring soil moisture state in the central U.S. does not influence the

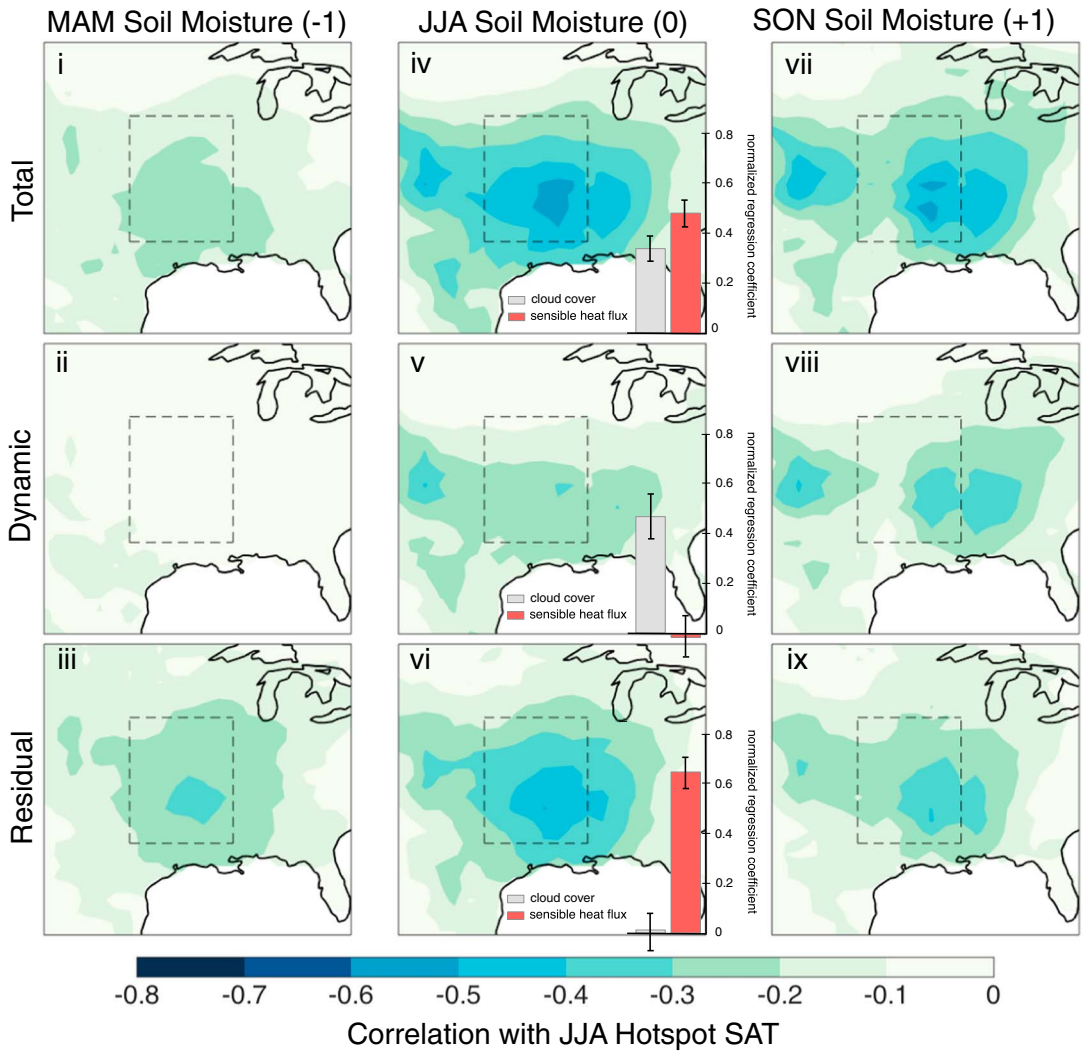

Figure 3. Correlation maps of (i, iv, vii) total, (ii, v, viii) dynamic, and (iii, vi, ix) residual JJA hot spot SAT with total column soil moisture at each grid point. The left column shows correlation with preseason (MAM) soil moisture, the middle with concurrent JJA soil moisture, and the right with postseason (SON) soil moisture. Normalized regression coefficients for JJA cloud cover (b_{cld}; gray) and sensible heat flux (b_{shf}; red) regressed on each component of JJA SAT are inlaid in Figures 3iv–3vi. Bars (whiskers) represent ensemble average (spread).

atmospheric circulation patterns that follow. Removing the influence of dynamics, however, leads to higher correlations between MAM soil moisture and JJA SAT (Figure 3iii). In fact, residual JJA hot spot SAT is more highly correlated with MAM soil moisture in the hot spot than total SAT is ($r = -0.36$). This supports our hypothesis that removing circulation-induced SAT variability allows us to better characterize SAT variability driven by the land surface feedback.

Instantaneous correlations in the hot spot are of similar magnitude for total and residual JJA SAT and JJA soil moisture, and dynamic SAT correlations remain weaker (Figures 3iv–3vi). Fall (September–November; SON) soil moisture is more highly correlated with JJA SAT and its components than MAM soil moisture is (Figures 3vii–3ix). Correlations of SON soil moisture with dynamic and residual hot spot SAT are of similar magnitude, which suggests that a hot summer dries soils in the hot spot whether the warm anomaly was circulation induced or land surface driven. To strengthen the case that residual hot spot SAT is land surface driven, we determine the relative influence of cloud cover and surface fluxes through a multivariate regression of the shortwave cloud radiative effect and the sensible heat flux on JJA hot spot SAT (bars inlaid in Figures 3iv–3vi). In each ensemble member, all fields are normalized by standard deviation at each grid point. A multivariate regression is then carried out at each grid point and the resulting normalized regression coefficients, b_{cld} and b_{shf}, are averaged over the hot spot to estimate relative contribution of clouds versus the land

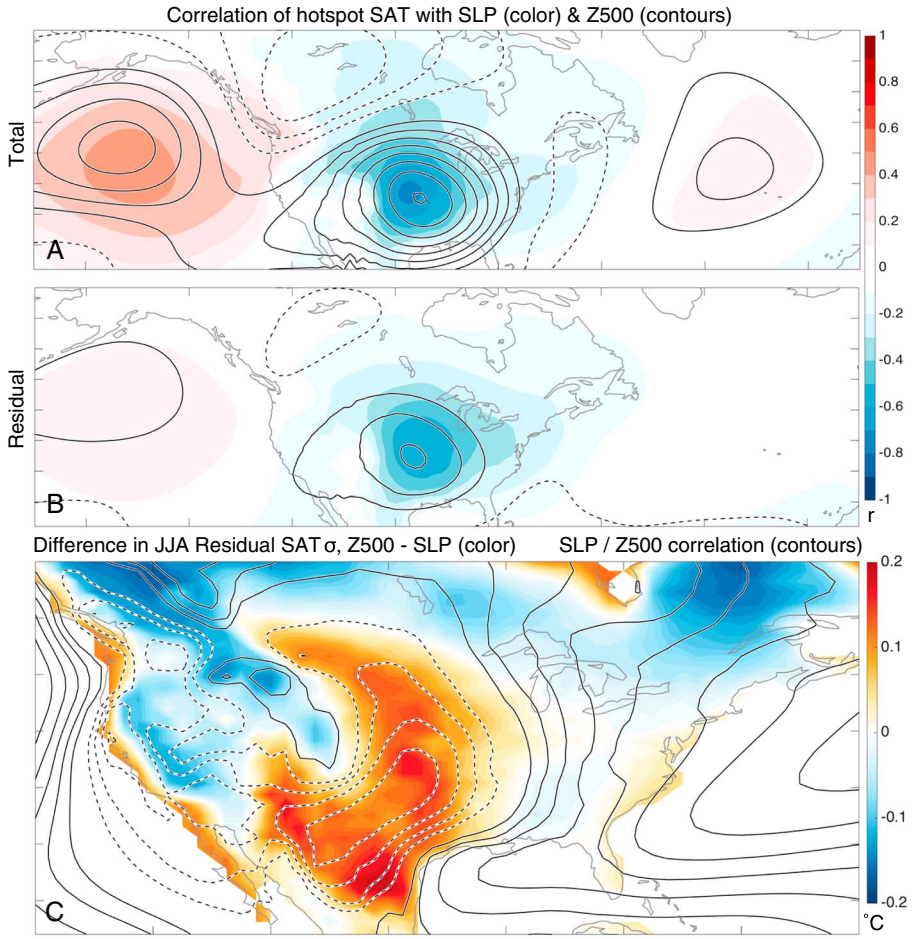

Figure 4. (a) Correlation map of total JJA hot spot SAT with SLP in color and with Z500 in contours. Z500 correlation contours range from 0.1 to 0.8 (solid) and −0.1 to −0.3 (dashed) in intervals of 0.1. (b) Same as Figure 4a, but with residual JJA hot spot SAT. (c) Difference in the standard deviation of JJA residual SAT (°C; color) using Z500 versus SLP to represent circulation. The residual SAT variability difference map is overlaid with a map of the correlation between SLP and Z500 (contours). Correlation contours range from 0.1 to 0.8 (solid) and −0.1 to −0.4 (dashed) in intervals of 0.1.

surface feedback. Bars in Figures 3iv–3vi show the average, and whiskers show the range in b_{cld} and b_{shf} across the ensemble. Cloud cover and the sensible heat flux play comparable roles in setting total JJA hot spot SAT, with an average b_{cld} of 0.34 and b_{shf} of 0.48 (Figure 3iv). This supports the narrative posited in Figure 1 that warm SAT anomalies in the hot spot occur in conjunction with clear skies, more incoming shortwave radiation, and an increased sensible heat flux. Regression on the components of JJA hot spot SAT confirm that variations in dynamic and residual SAT have different physical underpinnings. Dynamic SAT variability (Figure 3v) relates primarily to variations in cloud cover ($b_{cld} = 0.46$), as large cloud systems that impact radiation tend to be coupled to large-scale atmospheric circulation (Bony et al., 2015). Residual SAT variability (Figure 1vi) is primarily driven by variations in the sensible heat flux ($b_{shf} = 0.64$), which reflects the thermodynamic partitioning of surface fluxes by soil moisture in the hot spot region (Seneviratne et al., 2010). This illustrates the efficacy of dynamical adjustment in separating circulation induced from thermodynamic anomalies, as the method is able to reveal relationships between hot spot SAT and multiple aspects of the land surface feedback.

In winter, dynamic SAT and SLP are expected to show a quadrature relationship consistent with horizontal advection. In summer, surface lows form over hot, dry land surfaces and in regions of differential heating such as coastlines and are identifiable by a local anticorrelation between SAT and SLP (Rowson & Colucci, 1992). Because thermal lows are associated with local land surface conditions, their presence is not necessarily reflective of the large-scale circulation patterns that drive dynamic SAT. Over the ocean, the midlatitude atmosphere tends to feature SLP anomalies of the same sign as Z500 anomalies (Figure 4a). In the hot spot, positive (negative) correlations between JJA SAT and Z500 (SLP) are highest locally (Figure 4a). Low pressure

at the surface and high pressure aloft is representative of the atmospheric baroclinicity that sets up thermodynamically over hot, dry land surfaces. Dynamical adjustment removes covariability between hot spot SAT and Z500 as expected, both locally and remotely (Figure 4b). Correlations between residual hot spot SAT and SLP, however, remain almost unchanged over the hot spot region. After dynamical adjustment, local correlation between SAT and Z500 is reduced from 0.80 to 0.31 while local correlation between SAT and SLP is only reduced from −0.73 to −0.60. The magnitude of the remaining residual SAT-SLP correlation supports the thermodynamic interpretation of SAT variability in the hot spot region, that the state of the land surface (e.g., soil moisture) influences local SAT, which in turn sets up a spatially concomitant SLP signature. The remaining residual SAT-Z500 correlation is substantially reduced but not negligible, which is expected in a coupled system. The relationship may reflect the influence of large-scale circulation on soil moisture or vice versa (Fernando et al., 2016; Koster et al., 2016).

We have repeated the dynamical adjustment method using SLP (rather than Z500) as an indicator of circulation. Residual SAT σ from the two methods are compared in Figure 4c. More SAT variance is removed with SLP analogues than with Z500 analogues (i.e., Z500-derived residual σ is larger than SLP-derived residual σ) along the arc of the Great Plains, in the U.S. Southwest and Northern Mexico, and in coastal regions. These are regions where thermal lows are known to occur (Johnson, 2003) with feature of a negative correlation between Z500 and SLP (Figure 4c; dashed contours) representative of the baroclinic thermal low signature.

4. Summary

We have presented evidence that a method of dynamical adjustment developed by Deser et al. (2016) can be used to evaluate land surface-driven SAT variability in the CESM-LE. The dynamic and residual components of summer SAT are presented in terms of interannual variability, and the central U.S. hot spot of land surface-driven SAT is defined where residual variability accounts for more than half of the total JJA SAT variance. Temporal characteristics of the dynamic and residual (i.e., thermodynamic) hot spot SAT suggest that the latter is land surface driven. Finally, a general thermodynamic narrative is developed for residual SAT using the entire CESM-LE. Dynamical adjustment is able to reveal clear relationships between summer SAT and two key aspects of the land surface feedback (preseason soil moisture and sensible heat flux variability) that are normally obscured by the influence of atmospheric circulation. Dynamical adjustment performed with Z500 rather than SLP also leaves behind a thermodynamic, surface low signature that accompanies warm SAT in the hot spot. We conclude that dynamical adjustment can be used to empirically estimate the magnitude and spatial extent of land surface-driven SAT variability.

5. Discussion

Dynamical adjustment was previously employed to develop a physical understanding of SAT trends (Deser et al., 2016; Lehner, Deser, et al., 2017). The method also gives insight into interannual variability, allowing us to determine why one summer is hotter than another. Residuals tend to be larger in the summer than in the winter when horizontal advection plays a more prominent role in setting SAT (Deser et al., 2014; Sheffield et al., 2013). This does not necessarily mean that dynamical adjustment is not useful in the summer, just that thermodynamic processes play a role in setting SAT that is comparable in magnitude to dynamics. Determining the thermodynamic basis for the summer residual both validates dynamical adjustment as a method and indicates where land-atmosphere interactions may be meaningful.

We evaluate dynamical adjustment in a model, where there are thousands of years of simulation from which to pick analogues, and land surface information is temporally and spatially complete. Because dynamical adjustment is an empirical method, having as many analogues as possible is key to effectively characterizing circulation (van den Dool, 1994). Analogues may capture one aspect of circulation in the domain but have different features elsewhere and are therefore "imperfect." Additionally, care must be taken when using a linear method to explain features of a nonlinear coupled system. Land-atmosphere interactions are two way, which makes separating the forcing and response a challenge, particularly on monthly timescales (Levine et al., 2016). Further assessment of dynamical adjustment is warranted, particularly regarding its application to observational data sets (Lehner, Deser, et al., 2017). Temperature is a well-measured field, both spatially and temporally, while land surface observations tend to be limited. Developing a land-atmosphere hot spot definition based solely on temperature would allow us to leverage the observational record prior to the satellite era, ensuring robust statistics.

Acknowledgments
We thank Laurent Terray for conceiving the method of dynamical adjustment used in this study and Karen McKinnon, Adam Phillips, Nicolas Siler, and Jeffery Strong for helpful discussion. We also thank two anonymous reviewers for their constructive feedback. A. M. was supported by National Science Foundation (NSF) Graduate Research Fellowship Program under grant DGE-1144086 and the Graduate Student Visiting Fellowship at the National Center for Atmospheric Research. F. L. is supported by a Postdoc Applying Climate Expertise (PACE) fellowship cosponsored by NOAA and the Bureau of Reclamation. The CESM-LE simulations are available on the Earth System Grid (www.earthsystemgrid.org). The National Center for Atmospheric Research is sponsored by NSF.

References

Berg, A., Lintner, B. R., Findell, K. L., Malyshev, S., Loikith, P. C., & Gentine, P. (2014). Impact of soil moisture–Atmosphere interactions on surface temperature distribution. *Journal of Climate*, *27*, 7976–7993. https://doi.org/10.1175/JCLI-D-13-00591.1

Bony, S., Stevens, B., Frierson, D. M. W., Jakob, C., Kageyama, M., Pincus, R., … Webb, M. J. (2015). Clouds, circulation, and climate sensitivity. *Nature Geoscience*, *8*, 261–268. https://doi.org/10.1038/ngeo2398

Cheruy, F., Dufresne, J. L., Hourdin, F., & Ducharne, A. (2014). Role of clouds and land-atmosphere coupling in midlatitude continental summer warm biases and climate change amplification in CMIP5 simulations. *Geophysical Research Letters*, *41*, 6493–6500. https://doi.org/10.1002/2014GL061145

Dai, A., Trenberth, K., & Karl, T. (1999). Effects of clouds, soil moisture, precipitation, and water vapor on diurnal temperature range. *Journal of Climate*, 2451–2473. https://doi.org/10.1175/1520-0442(1999)012<2451: EOCSMP>2.0.CO;2

Delworth, T., & Manabe, S. (1993). Climate variability and land surface processes. *Advances in Water Resources*, *16*, 3–20. https://doi.org/10.1016/0309-1708(93)90026-C

Deser, C., Phillips, A., Alexander, M. A., & Smoliak, B. V. (2014). Projecting North American climate over the next 50 years: Uncertainty due to internal variability. *Journal of Climate*, *27*, 2271–2296. https://doi.org/10.1175/JCLI-D-13-00451.1

Deser, C., Phillips, A., Bourdette, V., & Teng, H. (2012). Uncertainty in climate change projections: the role of internal variability. *Climate Dynamics*, *38*, 527–547. https://doi.org/10.1007/s00382-010-0977-x

Deser, C. A., Terray, L., & Phillips, A. S. (2016). Forced and internal components of winter air temperature trends over North America during the past 50 years: Mechanisms and implications. *Journal of Climate*, *29*, 2237–2258. https://doi.org/10.1175/JCLI-D-15-0304.1

Durre, I., Wallace, J., & Lettenmaier, D. (2000). Dependence of extreme daily maximum temperatures on antecedent soil moisture in the contiguous United States during summer. *Journal of Climate*, *13*, 2641–2651. https://doi.org/10.1175/1520-0442(2000)013<2641:DOEDMT>2.0.CO;2

Feng, S., Hu, Q., & Oglesby, R. (2011). Influence of Atlantic sea surface temperatures on persistent drought in North America. *Climate Dynamics*, *37*, 569–586. https://doi.org/10.1007/s00382-010-0835-x

Fernando, D. N., Mo, K. C., Fu, R., Pu, B., Bowerman, A., Scanlon, B. R., … Zhang, K. (2016). What caused the spring intensification and winter demise of the 2011 drought over Texas? *Climate Dynamics*, *47*, 3077–3090. https://doi.org/10.1007/s00382-016-3014-x

Findell, K. L., & Eltahir, E. A. (2003). Atmospheric controls on soil moisture-boundary layer interactions. Part II: Feedbacks within the Continental United States. *Journal of Hydrometeorology*, *4*, 552–569. https://doi.org/10.1175/ 1525-7541(2003)004<0570:ACOSML>2.0.CO;2

Fischer, E. M., Rajczak, J., & Schär, C. (2012). Changes in European summer temperature variability revisited. *Geophysical Research Letters*, *39*, L19702. https://doi.org/10.1029/2012GL052730

Johnson, R. (2003). Thermal low. In J. Holton, J. Pyle, & J. Curry (Eds.), *Encyclopedia of Atmospheric Science* (pp. 2269–2273). London: Academic Press.

Kamae, Y., Shiogama, H., Imada, Y., Mori, M., Arakawa, O., Mizuta, R., … Ueda, H. (2016). Forced response and internal variability of summer climate over western North America. *Climate Dynamics*, *49*, 403–417. https://doi.org/10.1007/s00382-016-3350-x

Kay, J. E., Deser, C., Phillips, A., Mai, A., Hannay, C., Strand, G., … Vertenstein, M. (2015). The Community Earth System Model (CESM) Large Ensemble Project: A community resource for studying climate change in the presence of internal climate variability. *Bulletin of the American Meteorological Society*, *96*, 1333–1349. https://doi.org/10.1175/BAMS-D-13-00255.1

Koster, R., Chang, Y., Wang, H., & Schubert, S. (2016). Impacts of local soil moisture anomalies on the atmospheric circulation and on remote surface meteorological fields during boreal summer: A comprehensive analysis over North America. *Journal of Climate*, *29*, 7345–7364. https://doi.org/10.1175/JCLI-D-16-0192.1

Koster, R. D., Sud, Y. C., Guo, Z., Dirmeyer, P. A., Bonan, G., Oleson, K. W., … Xue, Y. (2006). GLACE: The Global Land-Atmosphere Coupling Experiment. Part I: Overview. *Journal of Hydrometeorology*, *7*, 590–610. https://doi.org/10.1175/JHM510.1

Kushnir, Y., Seager, R., Ting, M., Naik, N., & Nakamura, J. (2010). Mechanisms of Tropical Atlantic SST Influence on North American precipitation variability. *Journal of Climate*, *23*, 5610–5628. https://doi.org/10.1175/2010JCLI3172.1

Lehner, F., Deser, C., & Sanderson, B. (2016). Future risk of record-breaking summer temperatures and its mitigation. *Climatic Change*, 1–13. https://doi.org/10.1007/s10584-016-1616-2

Lehner, F., Deser, C., & Terray, L. (2017). Towards a new estimate of "time of emergence" of anthropogenic warming: Insights from dynamical adjustment and a large initial-condition model ensemble. *Journal of Climate*, *30*, 7739–7756. https://doi.org/10.1175/JCLI-D-16-0792.1

Lehner, F., Wahl, E. R., Wood, A. W., Blatchford, D. B., & Llewellyn, D. (2017). Assessing recent declines in Upper Rio Grande runoff efficiency from a paleoclimate perspective. *Geophysical Research Letters*, *44*, 4124–4133. https://doi.org/10.1002/2017GL073253

Levine, P. A., Randerson, J. T., Swenson, S. C., & Lawrence, D. M. (2016). Evaluating the strength of the land-atmosphere moisture feedback in Earth system models using satellite observations. *Hydrology and Earth System Sciences*, *20*(12), 4837–4856. https://doi.org/10.5194/hess-20-4837-2016

Lewis, S., & Karoly, D. (2013). Evaluation of historical diurnal temperature range trends in CMIP5 models. *Journal of Climate*, *26*, 9077–9089. https://doi.org/10.1175/JCLI-D-13-00032.1

Lorenz, R., Pitman, A. J., Hirsch, A. L., & Srbinovsky, J. (2015). Intraseasonal versus interannual measures of land-atmosphere coupling strength in a global climate model: GLACE-1 versus GLACE-CMIP5 experiments in ACCESS1.3b. *Journal of Hydrometeorology*, *16*, 2276–2295. https://doi.org/10.1175/JHM-D-14-0206.1

McKinnon, K. A., Rhines, A., Tingley, M. P., & Huybers, P. (2016). Long-lead predictions of Eastern US hot days from Pacific sea surface temperatures. *Nature Geoscience*, *9*, 389–394. https://doi.org/10.1038/ngeo2687

Merrifield, A., & Xie, S. (2016). Summer U.S. Surface air temperature variability: Controlling factors and AMIP simulation biases. *Journal of Climate*, *29*, 5123–5139. https://doi.org/10.1175/JCLI-D-15-0705.1

Miralles, D. G., Teuling, A. J., van Heerwaarden, C. C., & de Arellano, J. V.-G. (2014). Mega–heatwave temperatures due to combined soil desiccation and atmospheric heat accumulation. *Nature Geoscience*, *7*, 345–349. https://doi.org/10.1038/ngeo2141

Mueller, B., & Seneviratne, S. (2014). Systematic land climate and evapotranspiration biases in CMIP5 simulations. *Journal of Hydrometeorology*, *41*, 128–134. https://doi.org/10.1002/2013GL058055

Namias, J. (1982). Anatomy of great plains protracted heat waves (especially the 1980 U.S. summer drought). *Monthly Weather Review*, *110*, 824–838. https://doi.org/10.1175/1520-0493(1982)110<0824:AOGPPH>2.0.CO;2

Orth, R., & Seneviratne, S. (2017). Variability of soil moisture and sea surface temperatures similarly important for warm-season land climate in the community earth system model. *Journal of Climate*, *30*, 2141–2162. https://doi.org/10.1175/JCLI-D-15-0567.1

Perkins, S. E. (2015). A review on the scientific understanding of heatwaves-their measurement, driving mechanisms, and changes at the global scale. *Atmospheric Research*, *164*, 242–267. https://doi.org/10.1016/j.atmosres.2015.05.014

Romero-Lankao, P., Smith, J., Davidson, D., Diffenbaugh, N., Kinney, P., Kirshen, P., … Ruiz, L. V. (2014). North America. In V. Barros, et al. (Eds.), *Climate Change 2014: Impacts, Adaptation, and Vulnerability. Part B: Regional Aspects. Contribution of Working Group II to the Fifth Assessment Report of the Intergovernmental Panel on Climate Change* (pp. 1439–1498). Cambridge, UK: Cambridge University Press.

Rowson, D. R., & Colucci, S. J. (1992). Synoptic climatology of thermal low-pressure systems over southwestern North America. *International Journal of Climatology*, *12*, 529–545. https://doi.org/10.1002/joc.3370120602

Seneviratne, S., Corti, T., Davin, E., Hirschi, M., Jaeger, E., Lehner, I., … Teuling, A. (2010). Investigating soil moisture–climate interactions in a changing climate: a review. *Earth-Science Reviews*, *99*, 125–161. https://doi.org/10.1016/j.earscirev.2010.02.004

Sheffield, J., Camargo, S. J., Fu, R., Hu, Q., Jiang, X., Johnson, N., & Zhao, M. (2013). North American climate in CMIP5 experiments. Part II: Evaluation of historical simulations of intraseasonal to decadal variability. *Journal of Climate*, *26*, 9247–9290. https://doi.org/10.1175/JCLI-D-12-00593.1

Sippel, S., Zscheischler, J., Mahecha, M. D., Orth, R., Reichstein, M., Vogel, M., & Seneviratne, S. I. (2017). Refining multi-model projections of temperature extremes by evaluation against land-atmosphere coupling diagnostics. *Earth System Dynamics*, *8*, 387–403. https://doi.org/10.5194/esd-8-387-2017

Stegehuis, A. I., Teuling, A. J., Ciais, P., Vautard, R., & Jung, M. (2013). Future European temperature change uncertainties reduced by using land heat flux observations. *Geophysical Research Letters*, *40*, 2242–2245. https://doi.org/10.1002/grl.50404

Tawfik, A. B., Dirmeyer, P. A., & Santanello, J. A. (2015a). The heated condensation framework. Part I: Description and Southern Great Plains case study. *Journal of Hydrometeorology*, *16*, 1929–1945. https://doi.org/10.1175/JHM-D-14-0117.1

Tawfik, A. B., Dirmeyer, P. A., & Santanello, J. A. (2015b). The heated condensation framework. Part II: Climatological behavior of convective initiation and land-atmosphere coupling over the conterminous United States. *Journal of Hydrometeorology*, *16*, 1946–1961. https://doi.org/10.1175/JHM-D-14-0118.1

van den Dool, H. M. (1994). Searching for analogues, how long must we wait? *Tellus A*, *46*, 314–324. https://doi.org/10.1034/j.1600-0870.1994.t01-2-00006.x

Vogel, M. M., Orth, R., Cheruy, F., Hagemann, S., Lorenz, R., van den Hurk, B., & Seneviratne, S. (2017). Regional amplification of projected changes in extreme temperature strongly controlled by soil moisture-temperature feedbacks. *Geophysical Research Letters*, *44*, 1944–8007. https://doi.org/10.1002/2016GL071235

Wallace, J. M., Deser, C., Smoliak, B., & Phillips, A. (2015). Attribution of climate change in the presence of internal variability, In C.-P. Chang, et al. (Eds.), *Climate Change: Multidecadal and Beyond* (pp. 1–29). Singapore: World Scientific.

Wallace, J. M., Zhang, Y., & Renwick, J. A. (1995). Dynamic contribution to hemispheric mean temperature trends. *Science*, *270*, 780–783. https://doi.org/10.1126/science.270.5237.780

Yang, F., Kumar, A., & Lau, K. (2004). Potential predictability of US summer climate with perfect soil moisture. *Journal of Hydrometeorology*, *5*(5), 883–895. https://doi.org/10.1175/1525-7541(2004)005<0883:PPOUSC>2.0.CO;2

Zhang, J., Wang, W.-C., & Leung, L. R. (2008). Contribution of land-atmosphere coupling to summer climate variability over the contiguous United States. *Journal of Geophysical Research*, *113*, D22109. https://doi.org/10.1029/2008JD010136